



**HAL**  
open science

## CO<sub>2</sub> reforming in CH<sub>4</sub> over Ni/ $\gamma$ -Al<sub>2</sub>O<sub>3</sub> nano catalyst: Effect of cold plasma surface discharge

Loganathan Sivachandiran, Patrick da Costa, Ahmed Khacef

### ► To cite this version:

Loganathan Sivachandiran, Patrick da Costa, Ahmed Khacef. CO<sub>2</sub> reforming in CH<sub>4</sub> over Ni/ $\gamma$ -Al<sub>2</sub>O<sub>3</sub> nano catalyst: Effect of cold plasma surface discharge. Applied Surface Science, 2020, 501, pp.144175. 10.1016/j.apsusc.2019.144175 . hal-02429502

HAL Id: hal-02429502

<https://hal.science/hal-02429502v1>

Submitted on 20 Jul 2022

**HAL** is a multi-disciplinary open access archive for the deposit and dissemination of scientific research documents, whether they are published or not. The documents may come from teaching and research institutions in France or abroad, or from public or private research centers.

L'archive ouverte pluridisciplinaire **HAL**, est destinée au dépôt et à la diffusion de documents scientifiques de niveau recherche, publiés ou non, émanant des établissements d'enseignement et de recherche français ou étrangers, des laboratoires publics ou privés.



Distributed under a Creative Commons Attribution - NonCommercial 4.0 International License

## CO<sub>2</sub> reforming of CH<sub>4</sub> over Ni/ $\gamma$ -Al<sub>2</sub>O<sub>3</sub> nano catalyst: Effect of cold plasma surface discharge

L. Sivachandiran<sup>1,2\*</sup>, A. Khacef<sup>2</sup>, P. Da Costa<sup>3</sup>

<sup>1</sup>LPCP, Dept. of Chemistry, SRM Institute of Science and Technology, Chennai, India.

<sup>2</sup>GREMI, UMR 7344, CNRS-Université d'Orléans, 14 rue d'Issoudun, BP 6744, 45067 Orléans Cedex 02, France.

<sup>3</sup>Université Paris 6, UMR 7190 Sorbonne Univ-CNRS, Institut Jean Le Rond d'Alembert, 2 Pl Gare Ceinture, 78210, France.

**Keywords:** Ni/ $\gamma$ -Al<sub>2</sub>O<sub>3</sub> nanocatalyst, non-thermal plasma, CO<sub>2</sub> conversion, CH<sub>4</sub>

### Abstract

Modernization, deforestation and overwhelmingly growing world population are significantly increasing the atmosphere CO<sub>2</sub> level. The conversion of CO<sub>2</sub> to other products has attracted much more attention, especially atmospheric pressure cold plasma for CO<sub>2</sub> reforming of CH<sub>4</sub>. In this study the hydrogenation of CO<sub>2</sub> to CH<sub>4</sub> was carried out using Ni/ $\gamma$ -Al<sub>2</sub>O<sub>3</sub> nanocatalyst coupled non-thermal plasma dielectric barrier discharge reactor (NTP-DBD). The effect of temperature, plasma input power on CO<sub>2</sub> conversion rate and CH<sub>4</sub> selectivity have been studied. It was evidenced that, compared to conventional thermal catalysis (300 °C), plasma-catalysis has shown temperature shift (T shift) of 50 °C (250°C). Furthermore, at 250 °C, 10wt.%Ni/ $\gamma$ -Al<sub>2</sub>O<sub>3</sub> nanocatalyst has shown about 40% CO<sub>2</sub> conversion and 70% CH<sub>4</sub> selectivity with 340 J L<sup>-1</sup> input energy. At low operating temperature, increase in SIE increases the CO<sub>2</sub> conversion and CH<sub>4</sub> selectivity by about 10%. It is evidenced that the increase in CO<sub>2</sub> concentration in the feed significantly decreased the CO<sub>2</sub> conversion and increased the CO selectivity. The TEM analysis before and after catalytic experiments showed that the average "NiO" particle size is 7 and 10 nm, respectively. The plasma discharge slightly increases the particle size, however, it does not affect neither CO<sub>2</sub> conversion and nor CH<sub>4</sub> selectivity.

**Corresponding author at:** Laboratory of plasma chemistry and physics (LPCP), Department of Chemistry, SRM Institute of Science and Technology, Kattankulathur, Chennai-602203, India.

**E-mail address:** [sivachandiran.l@ktr.srmuniv.ac.in](mailto:sivachandiran.l@ktr.srmuniv.ac.in) (L. Sivachandiran)

## 1. Introduction

Modernization, deforestation and overwhelmingly increasing world population are significantly increasing the atmosphere CO<sub>2</sub> level [1,2]. As compared to pre-industrialization period, the atmosphere CO<sub>2</sub> concentration is already increased by 100 ppm [3]. The increase in atmospheric CO<sub>2</sub> concentration not only leads to global warming [4], but also affects the ecosystems [5]. The atmospheric CO<sub>2</sub> traps the heat from the earth surface; by this means it also increases the atmospheric water content by evaporating from the ocean. The atmospheric water contributes to 50% of the greenhouse effect. In addition, owing to the high level, CO<sub>2</sub> also dissolves in the ocean and increases the acidity and affects the ocean life. As a consequence, several methods have been developed to reduce the atmospheric CO<sub>2</sub> level. Annual decreases in CO<sub>2</sub> emission, over the next century, of 50% are required to stabilize the global temperature in its natural range [6].

The CO<sub>2</sub> mitigation can be divided in to two processes; (i) CO<sub>2</sub> capture and storage, and (ii) CO<sub>2</sub> conversion into value-added products [7,8,9]. Though the CO<sub>2</sub> capture and underground storage is energetically favoured, it has certain limitations like long time monitoring and possibility of ground water contamination. It is widely demonstrated that hydrogenation reaction is one of the most important chemical conversion of CO<sub>2</sub>. Furthermore, this reaction provides an excellent roadmap to sustainable development in the energy and environmental domain. Above all, this process not only reduces the amount of CO<sub>2</sub> released to the atmosphere but it also leads to production of fuels and valuable chemicals [10,11].

The hydrogenation of CO<sub>2</sub> into oxygenates and/or hydrocarbons (methane, methanol or dimethyl ether) have been the most investigated reactions to obtain fuels [12]. Among several hydrogenation reactions, methanation of carbon dioxide, following the Sabatier reaction, has more advantageous [13]. In addition, as methane is the main component of natural gas (NG), it can safely be transported using the existing NG infrastructures [14].

Several transition series metal oxides like Co, Ni, Mo and Pd have been studied for CO<sub>2</sub> activation reactions [15,16]. Nevertheless, Ni covers the larger part of the published works [17], since it is a cheaper metal, and economically viable as commercial standpoint. The main reported problem of Ni-based catalysts seems to be the deactivation at low temperature due to the interaction of the metal particles with CO and the formation of mobile nickel carbonyls that lead to the metal sintering [18, 19].

The CO<sub>2</sub> conversion at low operating temperature is desirable and economically feasible. In this regards, it is proposed that non-thermal plasma (NTP) discharge could be used to activate the catalyst at low temperature. The NTP is an ionised gas having mixture of highly active species like cation, anion and radicals [20,21]. Therefore, conversion of CO<sub>2</sub> by plasma discharge, especially non-thermal plasma (NTP) [22] and methanation [23,24] has been widely reported. Suib et al. [25]

demonstrated the CO<sub>2</sub> dissociation using atmospheric pressure rotating ac glow discharge reactor coated with Au, Pd, Pt and Rh metals. The maximum of 30.5% CO<sub>2</sub> conversion is reached with Rh coated rotator at 30 ml/min flow and 2.5% CO<sub>2</sub> in He as feed gas. In an another study, Benrabbah et al. [26] have reported that the CO<sub>2</sub> reforming of CH<sub>4</sub> using Nickel loaded-CeO<sub>2</sub>/ZrO<sub>2</sub> catalyst, and also found that the pre-treatment of catalyst with hydrogen plasma the catalyst showed higher CO<sub>2</sub> conversion with 5-8 W input power.

In this study, thermal catalysis, plasma, and plasma-catalysis processes have been investigated for direct hydrogenation of CO<sub>2</sub>. Activated  $\gamma$ -Al<sub>2</sub>O<sub>3</sub> and 10wt%.Ni/ $\gamma$ -Al<sub>2</sub>O<sub>3</sub> catalysts have been used for CO<sub>2</sub> reforming of methane reaction. The influence of catalyst loading, operating temperature and plasma input power on CO<sub>2</sub> conversion and CH<sub>4</sub> selectivity have been studied. The synergism between plasma and thermal catalysis has been explored.

## 2. Experimental

### 2.1. Non-thermal plasma (NTP) catalytic reactor

The general schematic of the packed bed NTP catalytic reactor employed for CO<sub>2</sub> hydrogenation is reported in Figure 1. The NTP-catalytic reactor is a cylindrical quartz tube characterized by 15 mm inner diameter, 1.5 mm thickness and 300 mm total length. In the center of the tube, a tungsten wire (0.9 mm thickness), used as a main electrode, was fixed by two ceramic rings. A copper grid, wrapped on the tube, was used as a ground electrode. The length of the ground electrode was fixed at 100 mm; the subsequent plasma discharge volume is 18 cm<sup>3</sup>.

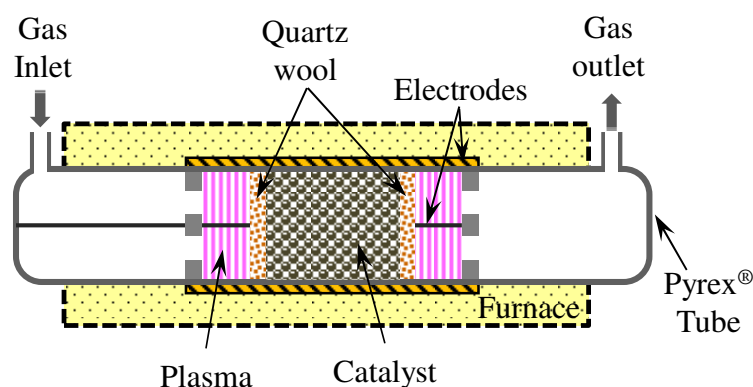


**Figure 1. General schematic of the NTP-catalytic, in-plasma catalytic (IPC), reactor.**

### 2.2. Non Thermal Plasma generation

The NTP was powered using a homemade sub-microsecond high voltage pulsed power supply unit (40 kV, 1 kHz), the details of this high-voltage generator have been reported elsewhere [27]. The applied pulsed voltage was varied between 12 and 29 kV, and the frequency was kept

constant as 100 Hz. The power delivered to the plasma reactor was measured by means of a voltage (Tektronix P6015A, 1000:1, 5 ns rise time) and a current (Pearson 4100, 1 V/A, 10 ns rise time) probes connected to a digital oscilloscope (Tektronix DPO 3054). The pulse energy ( $E_p$ ) was calculated by direct integration of the transient voltage and the current over one period.

### *2.3. Catalyst preparation and characterization*

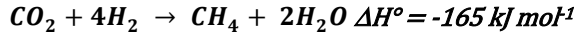
The Nickel supported catalysts were prepared by impregnating alumina beads (1 mm diameter, Sasol Germany GmbH), in metal precursor Nickel nitrate solution ( $\text{Ni}(\text{NO}_3)_2 \cdot 6\text{H}_2\text{O}$ ; Sigma-Aldrich). The suspension was stirred for 3 h at 50°C and at atmospheric pressure. The impregnated samples were dried at 120°C for 24 h, and then calcined at 500°C for 4 h at a heating rate of 3°C min<sup>-1</sup>, under air flow, to obtain the final form of the supported catalysts.

### *2.4. Experimental procedure*

For all the experiment, the total flow was fixed as 620 ml min<sup>-1</sup>, unless otherwise mentioned. It is worthy mention that the feed flow fixed in this study is 20 to 40 fold higher than the reported in the literature [28,29]. It is well established that, by decreasing the lower flow rate one can increase the gas residence time in the reaction zone, therefore, the CO<sub>2</sub> conversion could be increased significantly. Before each experiment, the catalyst was activated for 20 min at 400°C under H<sub>2</sub> (5%)/N<sub>2</sub> flow. The catalyst (1.5 g) was placed in the centre of the plasma discharge volume using quartz wool. This configuration is stated as In-plasma catalysis (IPC) and it leads to the two distinguished discharge configurations: gas phase streamer discharge before and after the catalyst bed, and surface discharge on the catalyst.

The exhaust gas, from the plasma reactor outlet, was first introduced into a condenser to separate the condensable product from the gas. The CO<sub>2</sub> conversion and CH<sub>4</sub> production have been studied for temperatures varied between 22 and 400°C. The reactor was placed in the tubular furnace and the set temperature was linearly increased at the rate of 5°C min<sup>-1</sup>. Before each experiment, the set temperature was maintained for 15 min after that, the plasma was ignited for 5 min. During plasma ignition, the furnace was turned off to avoid the electrical perturbation by plasma. The uncertainty of measured the temperature, during plasma treatment is  $\pm 5$  °C.

As mentioned in Equation 1, for the preliminary study, considering the stoichiometry balance, the CO<sub>2</sub> and H<sub>2</sub> ratio was fixed as 1:4. The concentration of CO<sub>2</sub>, CH<sub>4</sub>, CO, and O<sub>2</sub> was followed using a gas chromatography ( $\mu\text{GC}$ , MyGC - SRA). The sampling was performed each 3 min. In addition, gas analyzer (X-Stream, Emerson), equipped with TCD, IR, and UV detectors, was also used to follow the real time evolution of CO<sub>2</sub>, CH<sub>4</sub>, CO, H<sub>2</sub>, and C<sub>2</sub>H<sub>2</sub> concentration.



Equation 1

$$\text{CO}_2 \text{ Conversion (\%)} = \frac{[\text{CO}_2]_{\text{in}} - [\text{CO}_2]_{\text{out}}}{[\text{CO}_2]_{\text{in}}} \times 100$$

Equation 2

where  $[\text{CO}_2]_{\text{in}}$  and  $[\text{CO}_2]_{\text{out}}$  are  $\text{CO}_2$  inlet and outlet concentrations, respectively.

$$\text{CH}_4 \text{ Selectivity (\%)} = \frac{[\text{CH}_4]}{[\text{CO}_2 \text{ converted}]} \times 100$$

Equation 3

where,  $[\text{CH}_4]$  and  $[\text{CO}_2 \text{ converted}]$  are concentration of  $\text{CH}_4$ , at the reactor downstream, and the amount of  $\text{CO}_2$  converted, respectively.

### 3. Results and discussion

#### 3.1. Ni/ $\gamma\text{-Al}_2\text{O}_3$ characterization

The total surface area of the catalyst were determined by the multi-point Brunauer-Emmett-Tellet method (BET, Micromeritics ASAP 2010) using  $\text{N}_2$  as the sorbate at  $-196^\circ\text{C}$ . Before measurement, samples were outgassed at  $300^\circ\text{C}$  and  $5 \times 10^{-3}$  Torr pressure for 3 h. The BET measurement was performed, before ( $207 \text{ m}^2/\text{g}$ ) and after plasma treatment ( $190 \text{ m}^2/\text{g}$ ), and evidenced that there was no significant change in the total surface area. This finding shows that the plasma surface discharge did not change the catalyst surface morphology significantly.

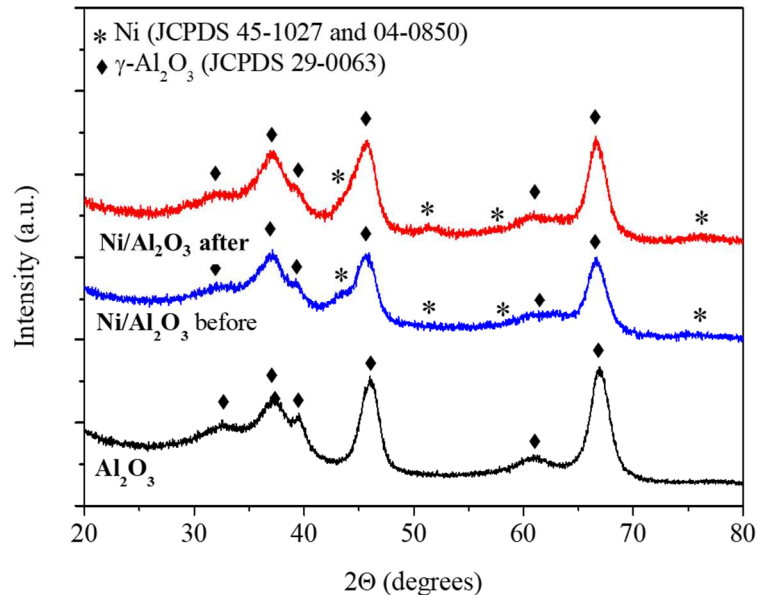
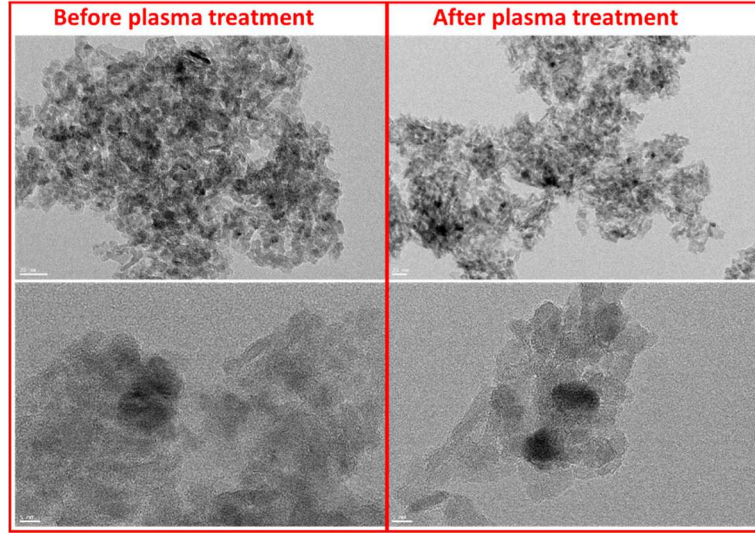


Figure 2. XRD pattern of 10wt%Ni/ $\gamma\text{-Al}_2\text{O}_3$  catalyst before and after plasma treatment.

As reported in Figure 2, the diffraction peak for Ni is too weak. This could be attributed to the very small crystal size of Ni. Moreover, no significant difference in XRD pattern is observed before

and after plasma treatment, and this is further confirmed by the surface morphology. The Transmission Electron Microscope (TEM) images of the catalyst, before and after plasma treatment, have been reported in Figure 3. It is observed that the average particle size of NiO, before plasma treatment, is about 8 nm. Indeed, after plasma treatment the average particle size is slightly increased to 10 nm. Thus, it can be concluded that the NiO nano particles have been dispersed on  $\gamma$ -Al<sub>2</sub>O<sub>3</sub> uniformly and the particle size does not significantly increase even after several hours of plasma treatment.



*Figure 3. TEM image of 10wt%.Ni/ $\gamma$ -Al<sub>2</sub>O<sub>3</sub> before and after plasma treatment.*

### 3.2. Cold plasma ignition and power characterization

All the experiments were performed at a constant frequency of 100 Hz and the energy deposition in the plasma reactor, the specific input energy (SIE), was evaluated for applied voltage between 12 and 29 kV. The SIE is determined using Equation 4.

$$SIE \left( \frac{J}{L} \right) = \frac{E_p (J) \cdot f (Hz)}{Q (L/s)} \quad \text{Equation 4}$$

Where  $f$  is the pulse repetition frequency,  $Q$  is the total gas flow rate at standard conditions, and  $E_p$  is the energy deposited into the plasma volume per current pulse. The pulsed energy  $E_p$  was determined through the time-resolved measurements of the applied voltage ( $U$ ) and discharge current ( $I$ ) and is given by Equation 5, where  $t$  is the pulse duration.

$$E_p (J) = \int_0^T U(t) \cdot I(t) \cdot dt \quad \text{Equation 5}$$

The evolution of SIE, as a function of applied voltage, is reported in Figure 4. It is observed that the SIE increases with increasing the applied voltage at constant frequency. The SIE is varied from  $92 \pm 12$  to  $489 \pm 12$  J. L<sup>-1</sup> when applied voltage varied from 12 to 29 kV. It is widely reported that with increasing the SIE, the plasma intensity and number of micro discharges could be increased [27]. Therefore, at high SIE, CO<sub>2</sub> conversion could be increased. However, reaching high CO<sub>2</sub> conversion with lower input energy with high gas flow rate is desirable.

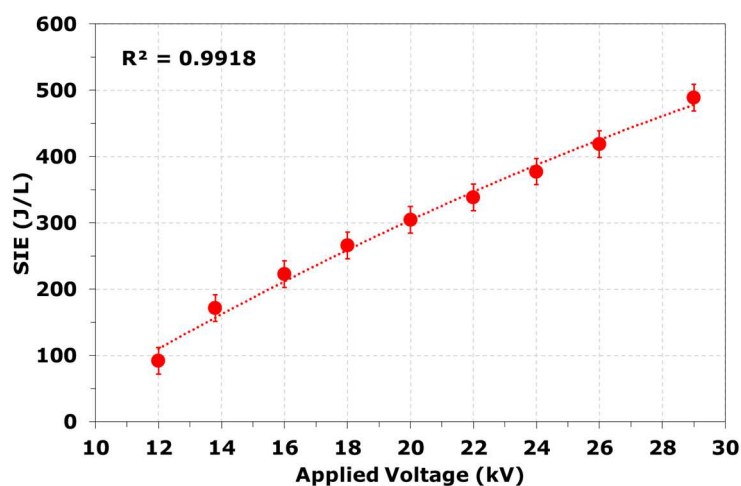


*Figure 4. Evolution of Specific Input Energy (SIE) as a function of applied voltage. Plasma is ignited at 620 ml.min<sup>-1</sup> constant flow rate and 100 Hz applied frequency.*

### 3.3. Thermal and plasma catalytic conversion of CO<sub>2</sub> over $\gamma$ -Al<sub>2</sub>O<sub>3</sub> catalyst

In order to understand the effect of  $\gamma$ -Al<sub>2</sub>O<sub>3</sub> packing on CO<sub>2</sub> decomposition by thermal and plasma discharge, the CO<sub>2</sub> conversion is determined for various conditions and reported in Figure 5. The thermal dissociation of CO<sub>2</sub> is not observed for empty reactor even at 400 °C. However, when plasma discharge is ignited with 340 J. L<sup>-1</sup> input energy, about 1% CO<sub>2</sub> is obtained at 250 °C with CO as the only product. Indeed, the CO<sub>2</sub> conversion remains constant with increase in temperature. This finding emphasizes the fact that without any catalysts in the plasma discharge zone CO<sub>2</sub> could be dissociated into CO.



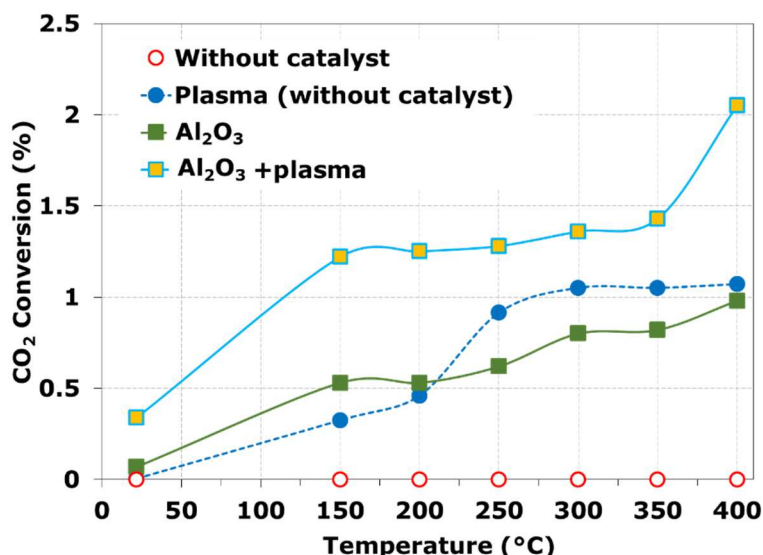
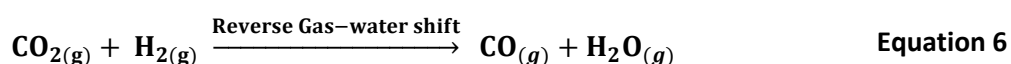


*Figure 5. CO<sub>2</sub> conversion as a function of temperature for empty and  $\gamma$ -Al<sub>2</sub>O<sub>3</sub> packed tubular reactors. Plasma discharge is ignited with 340 J. L<sup>-1</sup> at 640 ml.min<sup>-1</sup> constant flow rate (20% CO<sub>2</sub> + 80 H<sub>2</sub> mixture).*

As can be seen in Figure 5, if plasma discharge zone is packed with  $\gamma$ -Al<sub>2</sub>O<sub>3</sub>, as shown in Figure 1, thermal catalytic dissociation of CO<sub>2</sub> is observed at 150 °C. And then it gradually increases with increasing temperature and reached 1% at 400°C. It is worthy to mention that, for all the investigated temperature, only CO is quantified at the reactor outlet. Interestingly, when plasma is ignited on  $\gamma$ -Al<sub>2</sub>O<sub>3</sub> at 150 °C, about 1.2% CO<sub>2</sub> conversion is reached. The CO<sub>2</sub> conversion gradually increases with increasing temperature and at 400 °C about 2.2% is reached. This finding reveals the fact that, for CO<sub>2</sub> dissociation to CO, synergism could be exploited by coupling plasma and  $\gamma$ -Al<sub>2</sub>O<sub>3</sub> catalyst. However, the CO<sub>2</sub> conversion has to be significantly improved to with CH<sub>4</sub> formation rather than CO.



### 3.3. CO<sub>2</sub> conversion over 10wt%.Ni/ $\gamma$ -Al<sub>2</sub>O<sub>3</sub> catalyst

As reported in Equation 1, since CO<sub>2</sub> conversion is evidenced, along with the main products CH<sub>4</sub>, and H<sub>2</sub>O the intermediate CO has also been monitored. As can be seen in Figure 5, for the investigated temperature range  $\gamma$ -Al<sub>2</sub>O<sub>3</sub> as a catalyst, whether used alone or coupled with plasma, has shown less than 2% CO<sub>2</sub> conversion.

Indeed, as reported in Figure 6, 10wt% Ni doping on  $\gamma$ -Al<sub>2</sub>O<sub>3</sub> has significantly increased the CO<sub>2</sub> conversion. Similar results have also been reported by He et al. [30] on Ni-Al hydrotalcite catalyst. Thermal catalytic activity of 10 wt% Ni/ $\gamma$ -Al<sub>2</sub>O<sub>3</sub> catalyst begins above 250°C, and about 54% of CO<sub>2</sub> conversion is reached at 350°C. Under the similar operating conditions, when plasma discharge is coupled, the CO<sub>2</sub> conversion begins at 200°C, and 45% CO<sub>2</sub> conversion is reached at

250°C. The decrease in catalyst activation temperature can be attributed to the synergetic effect of plasma-catalyst coupling. Interestingly, for both operating conditions, the CO<sub>2</sub> conversion gradually decreases with increasing temperature. This can be attributed to the steam reforming of CH<sub>4</sub> to CO and H<sub>2</sub> at high temperature as reported in Equation 7 [31].

At 350°C, coupling of plasma discharge decreased the CO<sub>2</sub> conversion from 54 to 43%. This decrease in CO<sub>2</sub> conversion, at fixed temperature, can be attributed to the water gas shift reaction as reported in Equation 8. Even though this reaction needs high temperature, it can be suggested that owing to the non-thermal plasma surface discharge, local hotspot can be generated and CO could be converted back into CO<sub>2</sub>. Therefore, it can be concluded that, by plasma-catalyst coupling, the CO<sub>2</sub> can be converted at lower temperature than the conventional thermal catalytic process.

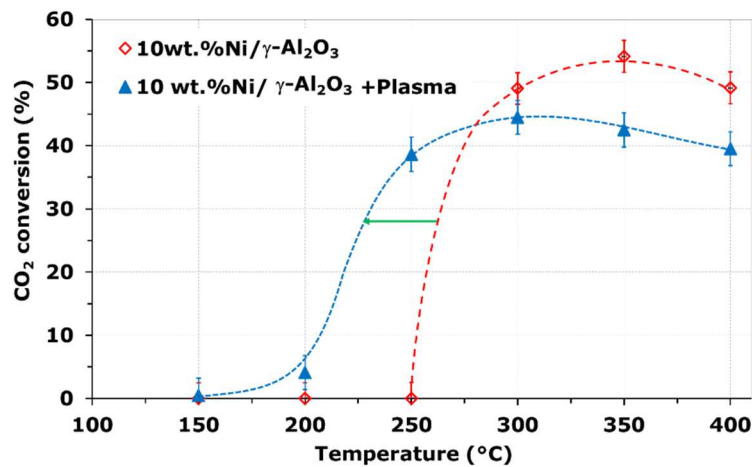
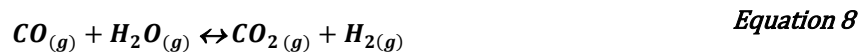
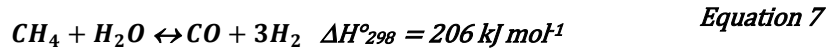


*Figure 6. CO<sub>2</sub> conversion as a function of temperature. Plasma discharge was ignited with a fixed specific input energy 340 J.L<sup>-1</sup>.*



It was evidenced that, without Ni doping on γ-Al<sub>2</sub>O<sub>3</sub>, CH<sub>4</sub> is not produced for all the investigated temperature. This result is in agreement with those reported by Jwa et al [32]. Authors have reported that the CO<sub>2</sub> conversion and CH<sub>4</sub> production increase with increasing the Ni content on β-zeolite. This implies that Ni doped on Al<sub>2</sub>O<sub>3</sub> are mainly involved in CO<sub>2</sub> hydrogenation processes. It can be suggested that although plasma dissociates CO<sub>2</sub> but it does not induce the hydrogenation reaction. The amount of CH<sub>4</sub> quantified at the reactor downstream, as a function of operating temperature, is reported in Figure 7.

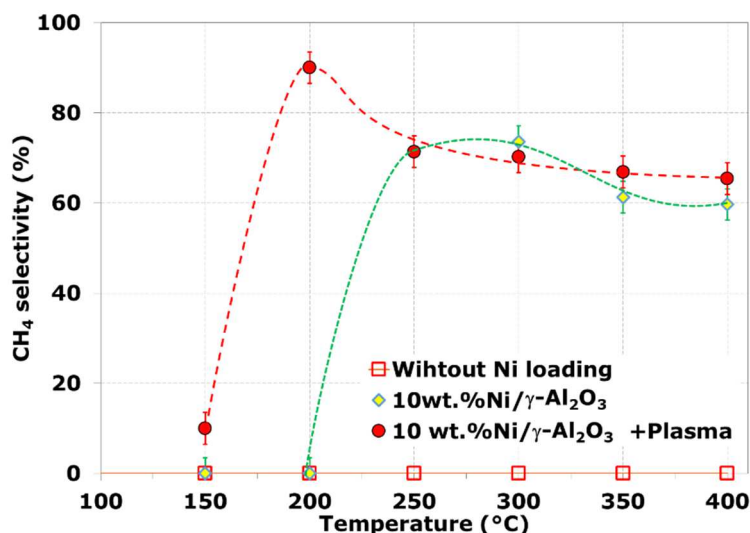


**Figure 7.** Amount of CH<sub>4</sub> produced as a function of temperature. Total flow of the feed gas was fixed at 640 ml min<sup>-1</sup> (20% CO<sub>2</sub> and 80% H<sub>2</sub>).

At 250°C, with or without plasma, 10 wt% Ni/γ-Al<sub>2</sub>O<sub>3</sub> catalyst has shown 70% CH<sub>4</sub> selectivity. As can be seen in Figure 7, CH<sub>4</sub> selectivity gradually decreases with increasing temperature. The following two hypotheses can be proposed for lower CH<sub>4</sub> selectivity, and decrease in CO<sub>2</sub> conversion with increase in temperature. (1) As reported in Equation 7, steam reforming of CH<sub>4</sub> to syngas (CO+H<sub>2</sub>), (2) the catalytic oxidation of CH<sub>4</sub> to CO<sub>2</sub>, CO, and H<sub>2</sub>O at high temperature [33].

The above suggested hypotheses were further evidenced, for both system, by monitoring the CO concentration as a function of temperature and reported in Figure 8. It is observed that, during thermal catalysis, increase in temperature increases the CO selectivity. Furthermore, the coupling of plasma increased the CO selectivity by two folds irrespective of the operating temperature. It was shown that at 300°C, CO selectivity of about 1.5% was obtained with 10 wt% Ni/γ-Al<sub>2</sub>O<sub>3</sub> catalyst. Indeed, when plasma is coupled, the CO selectivity increased two folds. This result supports the hypothesis of partial oxidation of CH<sub>4</sub> to CO and steam reforming of CH<sub>4</sub> to syngas by plasma discharge at high temperature.

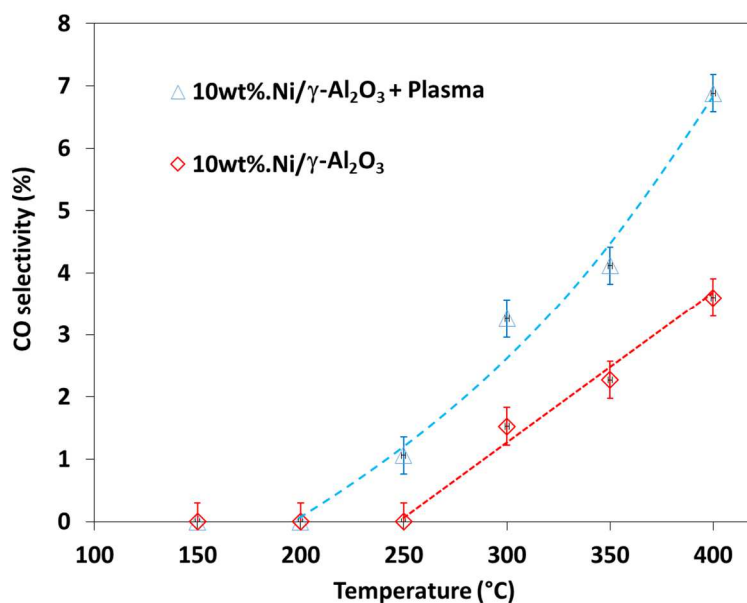


*Figure 8. CO quantified at the reactor downstream as a function of temperature for thermal and plasma catalytic conversion of CO<sub>2</sub> at 340 J L<sup>-1</sup> SIE.*

### 3.4. Effect of plasma injected power on CO<sub>2</sub> conversion and CH<sub>4</sub> selectivity.

As evidenced in the previous section, the coupling plasma discharge with thermal catalytic process enhances the CO<sub>2</sub> conversion and CH<sub>4</sub> selectivity at low temperature. However, above 300°C, the negative effect of plasma discharge is observed, i.e. decrease in CO<sub>2</sub> conversion and CH<sub>4</sub> selectivity. Therefore, in order to understand the effect of plasma input energy on CO<sub>2</sub> conversion and CH<sub>4</sub> selectivity, at 250°, the SIE was varied by varying the applied voltage at 100 Hz fixed frequency. The CO<sub>2</sub> conversion and CH<sub>4</sub> selectivity as a function of SIE is reported in Figure 9.

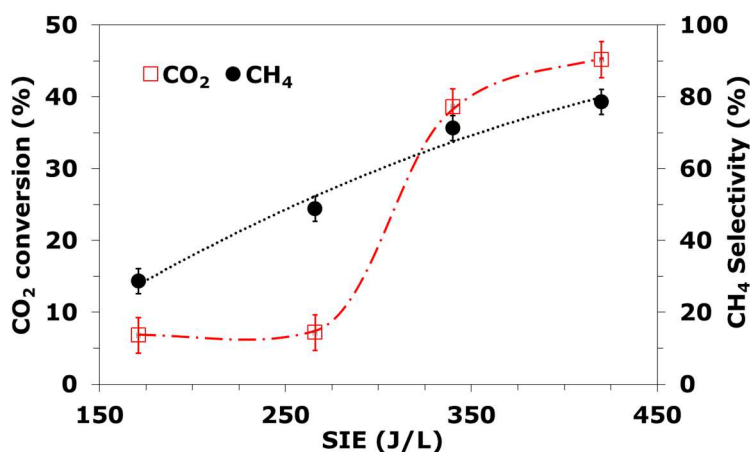


*Figure 9. CO<sub>2</sub> conversion and CH<sub>4</sub> selectivity as a function of plasma input energy. At 250°C, the SIE was varied between 170 and 420 J L<sup>-1</sup> by varying the applied voltage at fixed frequency of 100 Hz.*

As can be seen in Figure 9, the CH<sub>4</sub> selectivity increases from 30% to 80% with increasing SIE from 170 to 420 J L<sup>-1</sup>. This finding reveals the fact that at lower operating temperature high CH<sub>4</sub> selectivity could be achieved by increasing the SIE. Moreover, this is in line with the hypotheses

proposed in the previous section about lower CH<sub>4</sub> selectivity at high operating temperature. It is worth to mention that, at 250°C, by only thermal catalytic process insignificant CO<sub>2</sub> conversion is obtained. However, by coupling plasma about 7% CO<sub>2</sub> conversion is reached below SIE of 270 J L<sup>-1</sup>. Interestingly, the CO<sub>2</sub> conversion increased by fivefold and reached about 42% with increasing SIE from 270 to 340 J L<sup>-1</sup>. This finding emphasizes the fact that, at 250°C, by optimizing the SIE, the CO<sub>2</sub> conversion and CH<sub>4</sub> conversion could be improved significantly.

#### 4. Conclusions

Plasma-driven hydrogenation of CO<sub>2</sub> to CH<sub>4</sub> has been investigated for  $\gamma$ -Al<sub>2</sub>O<sub>3</sub> and 10wt% Ni/ $\gamma$ -Al<sub>2</sub>O<sub>3</sub> systems. At 250°C, the coupling of plasma with 10 wt% Ni/ $\gamma$ -Al<sub>2</sub>O<sub>3</sub> catalyst is significantly improved the CO<sub>2</sub> conversion and CH<sub>4</sub> selectivity. Under the given experimental conditions, about 45% CO<sub>2</sub> conversion is reached with CH<sub>4</sub> and CO selectivity of about 70 and 3%, respectively. Indeed, below 300°C, the synergetic effect of plasma-catalyst is observed for CO<sub>2</sub> conversion and CH<sub>4</sub> production. However, above 300°C, plasma-catalyst coupling favored the partial oxidation of CH<sub>4</sub> to CO<sub>2</sub>, CO, and H<sub>2</sub>O than that of CO<sub>2</sub> conversion to CH<sub>4</sub>. It was evidenced that, at high temperature, the increase of the plasma input power significantly increases the CO selectivity by favoring water gas reaction. The TEM image of NiO nano catalyst showed that, before and after plasma ignition, the particle size is not significantly increased. Thus it can be concluded that NTP discharge/catalyst coupling can be effectively used to convert CO<sub>2</sub> into CH<sub>4</sub> at low operating temperature.

#### References

- 
- [1] G.A. Olah, A. Goeppert, G.K.S. Prakash, *Journal of Organic Chemistry*, 74, 487 (2009).
  - [2] C. Song, *Catal. Today* 115 (2006) 2–32.
  - [3] D.M. Etheridge, L.P. Steele, R.L. Langenfelds, R.J. Francey, J.M. Barnola, V.I. Morgan, *Journal of Geophysical Research: Atmospheres*, 4115 (1996).
  - [4] Meehl, G. A.; Washington, W. M. *Nature* 1996, 382, 56. Sellers, P. J.; Bounoua, L.; Collatz, G. J.; Randall, D. A.; Dazlich, D. A.; Los, S. O.; Berry, J. A.; Fung, I.; Tucker, C. J.; Field, C. B.; Jensen, T. G. *Science* 1996, 271, 1402.
  - [5] S.C. Doney, V.J. Fabry, R.A. Feely, J.A. Kleypas, *Annual Review of Marine Science*, 1, 169 (2009).
  - [6] C. Azar, H. Rodhe, *Science*, 276 (1997) 1818-1919.
  - [7] J. Tollefson, *Nature*, 462 (2009) 966.
  - [8] G. Aydin, I. Karakurt, K. Aydiner, *Energy Policy*, 38 (2010) 5072–5080.
  - [9] J.A. Xu Moulijn, *Energy Fuels* 10 (1996) 305–325.
  - [10] P.G. Jessop, F. Joó, C.-C. Tai, *Coord. Chem. Rev*, 248 (2004) 2425–2442.
  - [11] W.M. Budzianowski, *Energy* 41 (2012) 280–297.

- 
- [12] K.M.K. Yu, I. Curcic, J. Gabriel, S.C.E. Tsang, *Chem Sus Chem* 1 (2008) 893–899.
- [13] T. Inui, T. Takeguchi, *Catal. Today* 10 (1991) 95–106.
- [14] K. Hashimoto, H. Habazaki, M. Yamasaki, S. Meguro, T. Sasaki, H. Katagiri, T. Mat-sui, K. Fujimura, K. Izumiya, N. Kumagai, E. Akiyama, *Mater. Sci. Eng.* 304–306(2001) 88–96.
- [15] J. Zhang, Z. Xin, X. Meng, Y. Lv, M. Tao, *Fuel*, (2014), 116, 25–33.
- [16] J. Sehested, K.E. Larsen, A.L. Kustov, A.M. Frey, T. Johannessen, T. Bligaard, M.P. Andersson, J.K. Nørskov, C.H. Christensen, *Top. Catal.* (2007), 45, 9–13.
- [17] W. Wang, J. Gong, *Front. Chem. Sci. Eng.* 5 (2011) 2–10.
- [18] S. E. Olesen, K. J. Andersson, C. D. Damsgaard, Ib Chorkendorff, *J. Phys. Chem. C*, (2017), 121, 15556–15564.
- [19] Y. Zhao, Y. Kang, H. Li, H. Li, *Green Chem.*, (2018), 20, 2781-2787.
- [20] U. Roland, F. Holzer, F. D. Kopinke, *Appl. Catal. B*, (2005), 28, 217–26.
- [21] F. Thevenet, L. Sivachandiran, O. Guaitella, C. Barakat, A. Rousseau, *J. Phys. D: Appl. Phys.*, (2014), 47, 224011.
- [22] D. Mei, X. Zhu, Y.L. He, J.D. Yan, X. Tu. *Plasma Sources Sci T*, (2015) 24, 015011.
- [23] L. He, Q. Lin, Y. Huang, *J Energy Chem*, 23 (2014) 587.
- [24] Liu, C-J, Xu, G., and Wang, T. (1999) *Fuel Process, Technol.*, 58, 119-134.
- [25] S. L. Suib, S. L. Brock, M. Marquez, J. Luo, H. Matsumoto, Y. Hayashi, *J. Phys. Chem. B*, 102 (1998) 9661-9666.
- [26] R. Benrabbah, C. Cavaniol, H. Liu, S. Ognier, S. Cavadias, M.E. Gálvez, P. Da Costa, *Catalysis Communications*, 89 (2017) 73-76.
- [27] L. Sivachandiran, A. Khacef, (2016), *RSC Adv.* 6, 29983–29995.
- [28] L. F. Spencer, A. D. Gallimore, *Plasma Chem Plasma Process*, (2011), 31, 79-89.
- [29] X. Fang, C. Peng, H. Peng, W. Liu, X. Xu, X. Wang, C. Li, W. Zhou, *ChemCatChem*, (2015), 7, 3753 – 3762.
- [30] L. He, Q. Lin, Y. Liu, Y. Huang, (2014), 23, 587-592.
- [31] C. j. Liu, J. Ye, J. Jiang, Y. Pan, *ChemCatChem*, (2011), 3, 529 – 541.
- [32] E. Jwa, S.B. Lee, H.W. Lee, Y.S. Mok, *Fuel Processing Technology*, (2013), 108, 89.
- [33] P. Da Costa, R. Marques, S. Da Costa, *Applied Catalysis B: Environmental* 84 (2008) 214–222.